PCCP

Accepted Manuscript

This article can be cited before page numbers have been issued, to do this please use: M. Muniz-Miranda, F. Muniz-Miranda and A. Pedone, *Phys. Chem. Chem. Phys.*, 2016, DOI: 10.1039/C5CP07597A.

ROYAL SOCIETY OF CHEMISTRY

www.rsc.org/pccp

View Article Online
DOI: 10.1039/C5CP07597A

Raman and DFT study of methimazole chemisorbed on gold colloidal nanoparticles

Maurizio Muniz-Miranda [1], Francesco Muniz-Miranda [2], Alfonso Pedone [2]*

[1] Department of Chemistry "Ugo Schiff", University of Florence, Via della Lastruccia 3, 50019 Sesto Fiorentino, Italy; *Email: muniz@unifi.it

[2] Department of Chemistry and Geology (DSCG), University of Modena and Reggio Emilia (UniMORE), Via Campi 103, 41125 Modena, Italy

*Corresponding Author; Email: muniz@unifi.it

ABSTRACT. The adsorption of methimazole on gold colloidal nanoparticles was investigated by combining surface-enhanced Raman scattering and density functional theory calculations, which allowed identifying the thiolate anion as the molecular species chemically interacting with the active sites of the gold surface, modeled as zero-charge metal adatoms, only through the sulfur atom. This result can be important for the use of these ligand/metal nanohybrids in the process of drug delivery. Moreover, functionalized gold nanoparticles are able to promote Raman enhancement in the red-light region as well as in the near-infrared, where generally no fluorescence emission occurs. This paves the way to the use of these nanosystems in biological environment, even *in vivo* experiments.

KEYWORDS: Methimazole; chemisorption; SERS; DFT; gold nanoparticles.

View Article Online
DOI: 10.1039/C5CP07597A

Introduction

Methimazole, commercially more known as tapazole (TZ), is a heterocyclic compound widely used in the treatment of hyperthyroidism,[1-3] mainly blocking the synthesis of thyroid hormones by impairing the oxidation of iodide to organic iodine. The therapeutic intake of TZ may nevertheless have hepatotoxic effects and cause serious adverse health effects, such as vasculitis, lupus erythematous syndrome, nephritis and thrombocytopenia.[4-6] The use of metal nanoparticles linked to drugs such as TZ can be useful in biomedical practice, following three possible actions: a) enhancing the therapeutic effect of the drug;[7-8] b) allowing efficient drug delivery, thanks to the carrier action played by metal nanoparticles, which can release the drug where it is needed;[9] c) increasing the therapeutic retention time in the circulation (relative to unpackaged drug).[10] The functionalized metal nanoparticles can therefore allow using a reduced dose of the drug with also more limited side reactions, which in the case of a long period of antithyroid therapy with methimazole can have severe consequences. Among the metal nanoparticles, those consisting of gold provide best biomedical use for at least two reasons: the low toxicity in comparison to those of other noble metals; the absence of alterations due to oxidative processes. The study of the interaction between TZ and gold nanoparticles in colloidal suspension is therefore particularly important for understanding the properties of these molecule-metal nanohybrids. This present investigation is performed with the help of the SERS spectroscopy, which provides enormous intensification of the Raman bands of molecules adsorbed on nanostructured surfaces of metals such as silver, gold and copper.[11]A long- and a short-range mechanisms are generally proposed in the explanation of the SERS effect: according to the former one, the molecule, by adhering to the metal, undergoes an electric field much larger than that far from the surface, whereas for the

View Article Online
DOI: 10.1039/C5CP07597A

latter one the polarizability tensor of the ligand is perturbed by the formation of chemical bonds or by a charge-transfer process with the metal. The electromagnetic mechanism is accepted contributing predominantly to the Raman enhancement, usually up to 10^6 factors, whereas the enhancement factor due to the chemical effect is much smaller (at most two orders of magnitude), but its influence on the SERS spectral pattern can be fundamental for identifying the molecular sites involved in the chemical interaction with the substrate. The interpretation of the SERS data can be efficiently performed on the basis of DFT calculations,[12-14] in order to understand the type and strength of the interaction of the molecule with the active sites of the metal surface. We also want to explore the possibility to obtain FT-SERS spectra using excitation in the NIR spectral region, which coincides with the biological transparency window where generally fluorescence emission does not occur. This could allow the use of SERS spectroscopy in biomedicine to recognize the presence of the drug both *in vitro* and *in vivo*.

Experimental

Preparation of metal colloids

Gold colloids were prepared by reduction of tetrachloroauric acid (Aldrich, purity 99.9%) with excess sodium citrate (Aldrich, purity 99%) according to the Turkevich's procedure.[15] The usual pH value of the gold colloidal dispersion was about 6. Methimazole (TZ), furnished by Fluka (purity ≥99%), was added to Au colloidal suspensions obtaining 10^{-5}M concentration. Some drops of Au/TZ colloid were deposited and dried on aluminium plate for microRaman measurements.

View Article Online
DOI: 10.1039/C5CP07597A

Raman measurements

Raman spectra of TZ as solid sample, dissolved in neutral and alkaline aqueous solutions or adsorbed on Au colloidal nanoparticles were collected with a Fourier transform (FT)-Raman spectrometer (Bruker Optics, Model MultiRam), equipped with a broad range quartz beamsplitter, an air-cooled Nd:YAG laser excitation source (1064 nm) and a Ge diode detector cooled with liquid nitrogen. The instrument provided a spectral range of 3600–50 cm^{-1} (Stokes shift). The experiments were performed in a 180° geometry, with 200 mW of laser power.

Raman spectra of TZ in Au colloids were recorded using the 647.1-nm line of a Coherent Krypton ion laser and a Jobin-Yvon HG2S monochromator equipped with a cooled RCA-C31034A photomultiplier. The experiments were performed with a defocalized laser beam in a 90° geometry, with 50 mW of laser power, in order to impair thermal effects that may provoke degradation of the sample and/or poor spectral reproducibility. Power density measurements were performed with a power meter instrument (model 362, Scientech, Boulder, CO, USA) giving ~5% accuracy in the 300-1000 nm spectral range.

Raman spectra of the Au/TZ colloidal samples deposited on Al plate were recorded by using a microRaman spectrometer RM 2000 Renishaw equipped with a diode laser emitting at 785 nm and a single grating monochromator. Sample irradiation was accomplished by using the 50×microscope objective of a Leica Microscope DMLM. The beam power was ~3mW, and the laser spot size was adjusted between 1 and 3 mm. The backscattered Raman signal was filtered by a double holographic Notch filter system and detected by an air-cooled CCD (2.5 cm^{-1}per pixel). All spectra were calibrated with respect to a silicon wafer at 520 cm^{-1}.

UV-visible absorption measurements

View Article Online
DOI: 10.1039/C5CP07597A

Absorption spectra of the gold colloidal suspensions were observed in the 200-1100 nm spectral region by means of a Cary 5 Varian spectrophotometer.

XPS measurements

X-Ray Photoelectron Spectroscopy (XPS) measurements were performed using a non-monochromatic Mg Kα X-ray source (1,253.6 eV) and a VSW HAC 5000 hemispherical electron energy analyzer operating in the constant-pass-energy mode at E_{pas}= 44 eV. The samples were prepared just before the analysis by depositing few drops of the colloidal suspensions on soda glass substrates and letting the solvent to evaporate. In order to increase the amount of metal nanoparticles (NPs) deposited on the surface, this procedure was repeated several times. Then, the NPs-loaded glasses were introduced in the UHV system via a load lock under inert gas (N_2) flux, and kept in the introduction chamber overnight allowing the removal of volatile substances, as confirmed by the achieved pressure value ($2x10^{-9}$ mbar), just above the instrument base pressure. The obtained spectra were referenced to C 1s core peak at 284.8 eV assigned to the adventitious carbon. The spectra were fitted using XPS Peak 4.1 software vers. 2.3.15, employing Gauss-Lorentz curves after subtraction of a Shirley-type background.

Computational details

All calculations were carried out by means of the Gaussian 09 package[16] using the B3LYP[17,18] hybrid exchange and correlation functional along with the def2TZVPP combined pseudopotential and basis set.[19-21] This basis set has been adopted here because it performs better than the more commonly used LANL2DZ. This latter is usually employed for metal-ligand nanohybrids (for example, refs 13,22-25), because it is a rather good compromise between

View Article Online
DOI: 10.1039/C5CP07597A

accuracy and computational burden: it is a double-zeta basis set, with no polarization functions added. For this work, instead, we decided to use a more complex and computationally demanding basis set: def2TZVPP is a triple zeta basis set and has two polarization functions added. Previously, some of us proved that it performed better than LANL2DZ concerning structures and optical properties of noble metal-based nanoclusters.[26,27] We have also performed a test by comparing the B3LYP/def2TZVPP and B3LYP/LANL2DZ results for the Au_2 cluster: def2TZVPP was more accurate than LANL2DZ in reproducing both the experimental Au-Au bond length and the bonding energy, as shown in **Table S4 (ESI)**.

The molecular structures and the vibrational frequencies of TZ and of the Au/TZ model systems were computed adopting tight convergence criteria of Gaussian 09. By allowing all the parameters to relax, the optimized geometries corresponded to true energy minima, as revealed by the lack of imaginary values in the vibrational mode calculations.

Raman spectra in aqueous solution

The study of the TZ interaction with gold nanoparticles is complicated by the tautomerism of the molecule. **Fig. 1** shows the DFT-optimized structures of TZ, such as thione and thiol, depending on whether the hydrogen atom is linked to the nitrogen atom of the heterocycle or to the sulfur atom bonded to the ring. In the solid state TZ is present as thione, as reported for the crystal structure obtained by X-ray diffraction.[28] The Raman spectrum of solid TZ is shown in **Fig. 2**, along with the Raman spectrum in aqueous solution at neutral pH, which much resembles the Raman spectrum of the solid, in the number and position of the bands as well as in the relative

View Article Online
DOI: 10.1039/C5CP07597A

intensities. On the other hand, nothing highlights in the 2500-2600 cm^{-1} spectral region the presence of a Raman band due to the S-H stretching mode of the thiolic form.

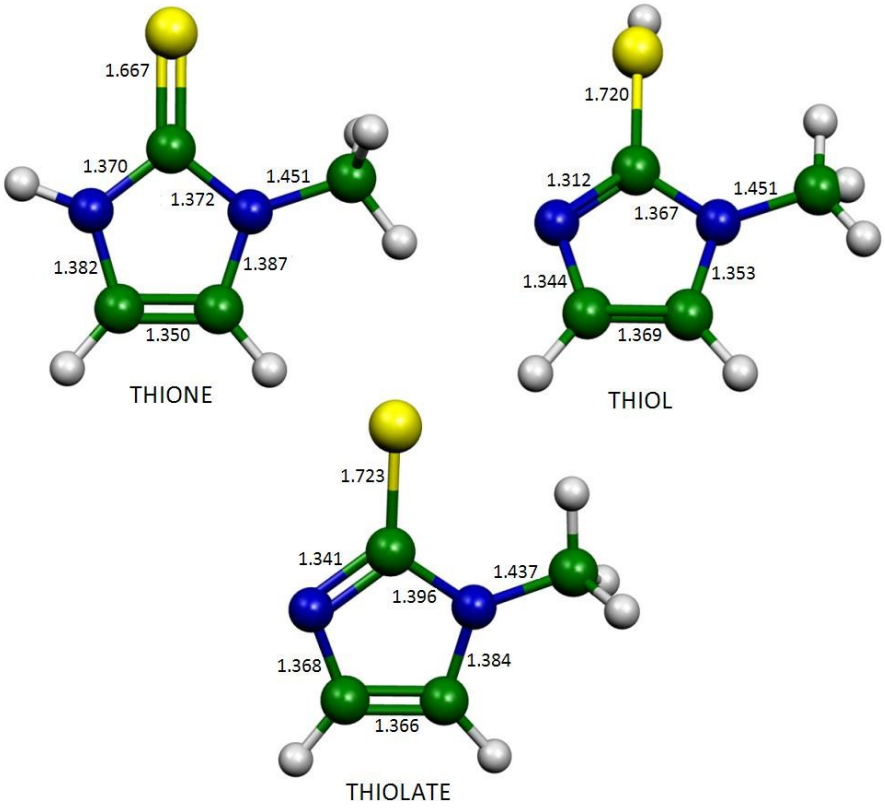

Fig. 1 – Optimized structures of TZ (thione and thiol) and TZA (thiolate anion).

Therefore, it is to be assumed that in neutral aqueous solution TZ is predominantly present as thione, as well as in the solid. This conclusion finds validation in the DFT calculations: i) thione results more stable than thiol, with free energy difference ΔG = 8.11 kcal/mol; ii) the calculated vibrational frequencies of TZ as thione reproduce much better those observed (see **Table S1**, **ESI**). A description of the normal modes of TZ as thione in terms of atomic Cartesian displacements is shown in **Fig. S1 (ESI)** for the prominent Raman bands observed in neutral aqueous solution. These modes are mainly attributable to in-plane ring deformations or to bending motions of the methyl group.

View Article Online
DOI: 10.1039/C5CP07597A

SERS spectra in gold colloids

There is the possibility that TZ adsorbs on Au colloidal nanoparticles as thiolate anion (TZA), despite that the pKa of the molecule in water is 11.38.[29] It has already been suggested that TZ adsorbs on silver in the thiolate form on the basis of SERS studies in Ag colloidal suspensions.[25] The structure of the thiolate anion is shown in **Fig. 1,** while the comparison between Raman and calculated frequencies is reported in **Table 1**. A description of the normal modes of TZA in terms of atomic Cartesian displacements is shown in **Fig. S2 (ESI)** for the prominent Raman bands observed in alkaline aqueous solution. These modes are mainly attributable to in-plane ring deformations or to bending motions of the methyl group.

Thiolate could bind to gold through the sulfur atom and/or the sp^2 nitrogen atom of the ring. Both atoms can be considered sites potentially deputies for the molecular interaction with the metal, having largely negative partial charges. **Table S2 (ESI)** shows the atomic partial charges as deriving from the analysis of the Mulliken and Hirshfeld populations[30] for all the calculated molecular species. In both population analyses the electronic charge of the thiolate anion results partially transferred to the rest of the molecule, even though the sulfur atom maintains the largest negative charge. The Raman spectrum of TZ in alkaline aqueous solution (pH> 12), attributable to thiolate, appears to be very different from the Raman spectrum in neutral solution (**Fig. 2**); in particular the band at about 1360 cm^{-1} is largely predominant, whereas that around 700 cm^{-1} strongly decreases in intensity in comparison with the corresponding one in neutral solution. Finally, in the 1400-1500 cm^{-1} region no strong band appears, while the band at higher frequency, around 1580 cm^{-1}, is missing.

View Article Online
DOI: 10.1039/C5CP07597A

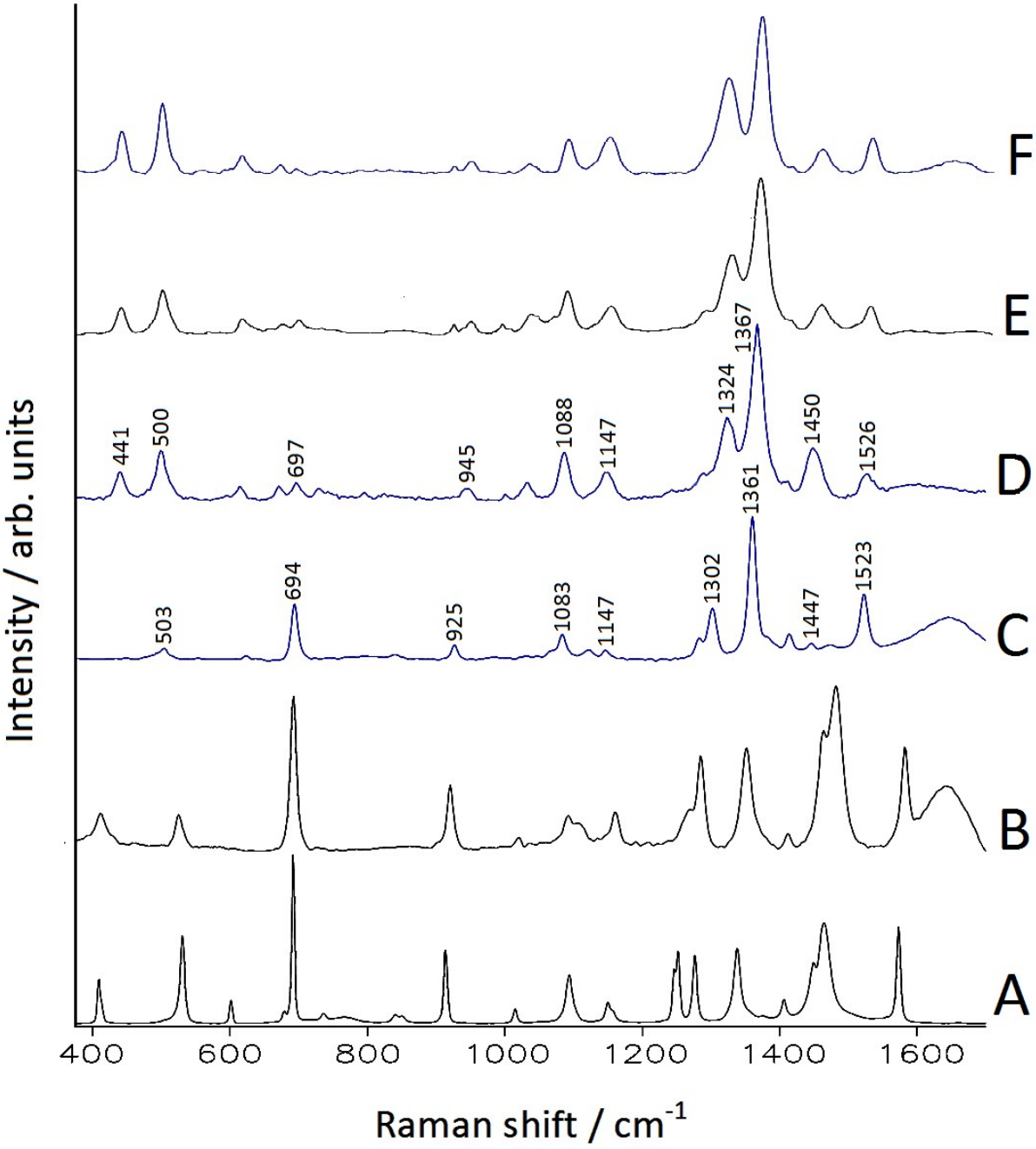

Fig. 2 – Raman spectra of TZ as solid sample (A), in neutral (B) and alkaline (C) solution (10^{-1}M concentration). The SERS spectra of TZ in Au colloid (10^{-5} M concentration) obtained by different laser excitations (D: 647.1 nm; E: 785 nm; F: 1064 nm) are reported for comparison.

View Article Online
DOI: 10.1039/C5CP07597A

SERS spectra of TZ in silver colloids were analyzed by Biswas *et al.*,[25] who proposed chemisorption of the ligand through both the sulfur atom and the ring nitrogen atom of the thiolate anion. SERS spectra in gold colloids, instead, are not reported so far in the literature. **Fig. 2** shows the comparison of the SERS spectra of TZ in Au colloid, obtained with different exciting lines, with the Raman spectra of the molecule in aqueous solutions. It is evident that the SERS spectra do not correspond to the Raman spectrum of the molecule in neutral solution, where TZ is present as thione, while they resemble that of the alkaline solution, where the thiolate anion (TZA) is predominant. In particular, the most intense SERS band at 1367 cm^{-1} is very close to the strongest Raman band observed in alkaline solution at 1361 cm^{-1}.

The UV-visible absorption spectrum of the gold colloid after addition of TZ in low concentration (10^{-5}M) undergoes dramatic changes with respect to the absorption spectrum of the free-ligand colloid, which shows the plasmon band of the non-aggregated gold nanoparticles at about 520 nm (see **Fig. 3**). This latter band decreases drastically by adding TZ, while a new intense plasmon band appears, due to aggregated gold particles, with a maximum around 700 nm, but extending well beyond the visible region, until the near-infrared region. This aggregation can be attributed to the effect of chemisorbed TZ molecules, which alters the zeta potential of the gold nanoparticles. This interpretation can be explained on the basis of the paper by M.E. Reeves and coworkers,[31] which analyzed the aggregation of gold nanoparticles induced by binding to small molecules. Actually, gold nanoparticles, prepared by citrate reduction of chloroauric acid, are electrostatically stabilized by adsorbed citrate anions and negatively-charged byproducts, leading to a largely negative zeta potential, which prevents aggregation. The particle aggregation observed in the UV-vis absorption spectra of gold colloidal suspensions after addition of thiols, dithiols, or amino acids was attributed to the binding of these ligands to the gold surface.

View Article Online
DOI: 10.1039/C5CP07597A

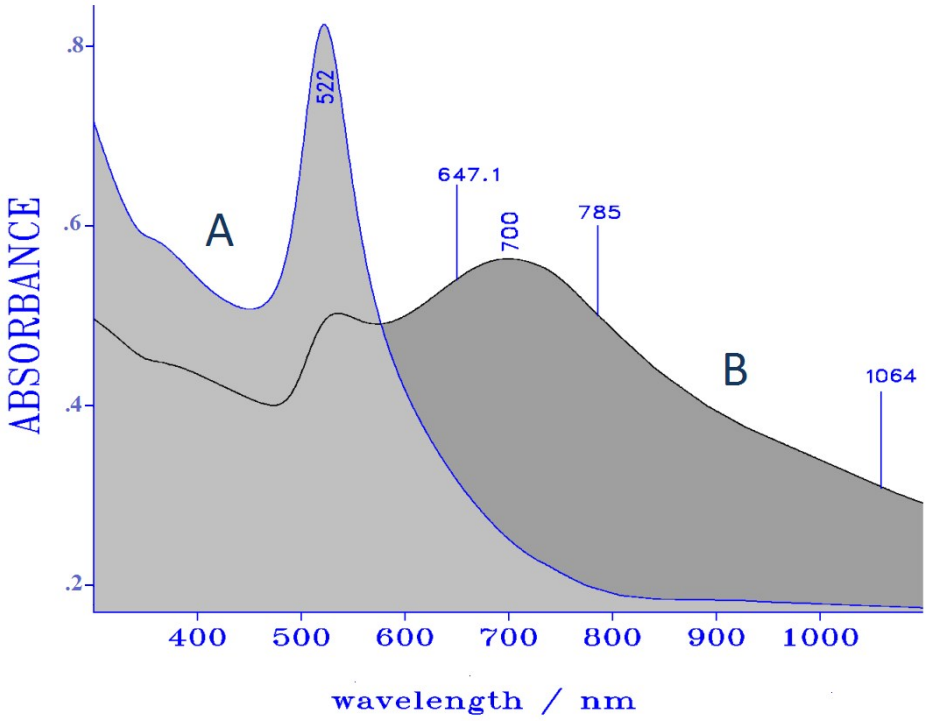

Fig. 3 – UV-vis-NIR absorption spectra of Au colloids in the absence (A) and in the presence of 10^{-5} M TZ (B). The wavelengths of the laser lines used for the Raman excitation (647.1, 785, 1064 nm) are shown.

In particular, the thiol groups are able to form strong, covalent bonds with the gold nanoparticles, reducing the absolute value of the zeta potential and promoting aggregation. These findings, reported in the Reeves' paper, are perfectly suited to the situation shown in our work, because our gold nanoparticles are obtained by citrate reduction and the TZ molecules have thiol groups suitable to the chemical interaction with gold. As a conclusion, the absorption spectrum of the Au colloid after addition of TZ strongly suggests the chemisorption of the ligand molecules on the gold surface. This, however, is to be confirmed by a detailed analysis of the SERS data.

Fig. 3 shows the wavelength positions of the laser radiations used in the present work for obtaining SERS spectra. By excitation at 647.1 nm, as well as at 785 nm, and even at 1064 nm,

View Article Online
DOI: 10.1039/C5CP07597A

an efficient SERS response is obtained, with spectra quite comparable to each other in both band positions and relative intensities, as shown in **Fig. 2**. For the first two exciting lines, the SERS activity can be attributed to a resonance between the laser radiation and the plasmon band of the aggregated gold particles, where the ligand molecules are adsorbed; for the excitation with laser line at 1064 nm, which is far from the maximum of the plasmon band, it could be due, more than to the electromagnetic mechanism related to the plasmon resonance, to the effect of the chemical interaction between molecule and metal, as suggested by the occurrence of the plasmon band at 700 nm. The chemical enhancement mechanism can also act in the SERS spectra recorded by laser excitation at 647.1 and 785 nm, where however the effect of electromagnetic enhancement is expected to be predominant due to the resonance with the plasmon band.

In **Table 1** the SERS wavenumbers are compared with those Raman in alkaline solution: no large frequency-shift is detected by interaction with the metal, with the exception of the weak Raman band at 925 cm^{-1}, which moves to 945 cm^{-1} in the SERS, and that at 1302 cm^{-1}, which shifts to 1324 cm^{-1}. The SERS band at 1367 cm^{-1} is the most intense of the spectrum, as well as the corresponding Raman band at 1361 cm^{-1}, while the two low-frequency SERS bands, especially that at 500 cm^{-1}, markedly increase in intensity.

The DFT computational approach .with ligand bound to adatoms or adclusters constituted by one or few metal atoms cannot reproduce the electromagnetic SERS enhancement, for which it should be necessary to model the metal surface, but it is generally sufficient to simulate the SERS profile of a chemisorbed species, including band positions and relative intensities.[12-14,32-34] In addition, these DFT calculations can provide information on the type of adsorbed species, on the molecular sites of interaction with the substrate and also on the adsorption geometry. In our case, the species that may adsorb on the surface of the Au colloidal nanoparticles is the molecule

View Article Online
DOI: 10.1039/C5CP07597A

TZ, in thione form as in neutral aqueous solution, or the thiolate anion TZA formed by deprotonation of TZ, as hypothesized by adsorption on silver.[25] In the first case, the adsorption is expected occurring via the lone-pair of the sulfur atom; in the second one, there are two possible sites of adsorption, the sulfur atom and the sp^2 nitrogen atom of the ring. Therefore, for the DFT calculations we have proposed different ligand/metal complexes, whose optimized structures are shown in **Fig. 4**.

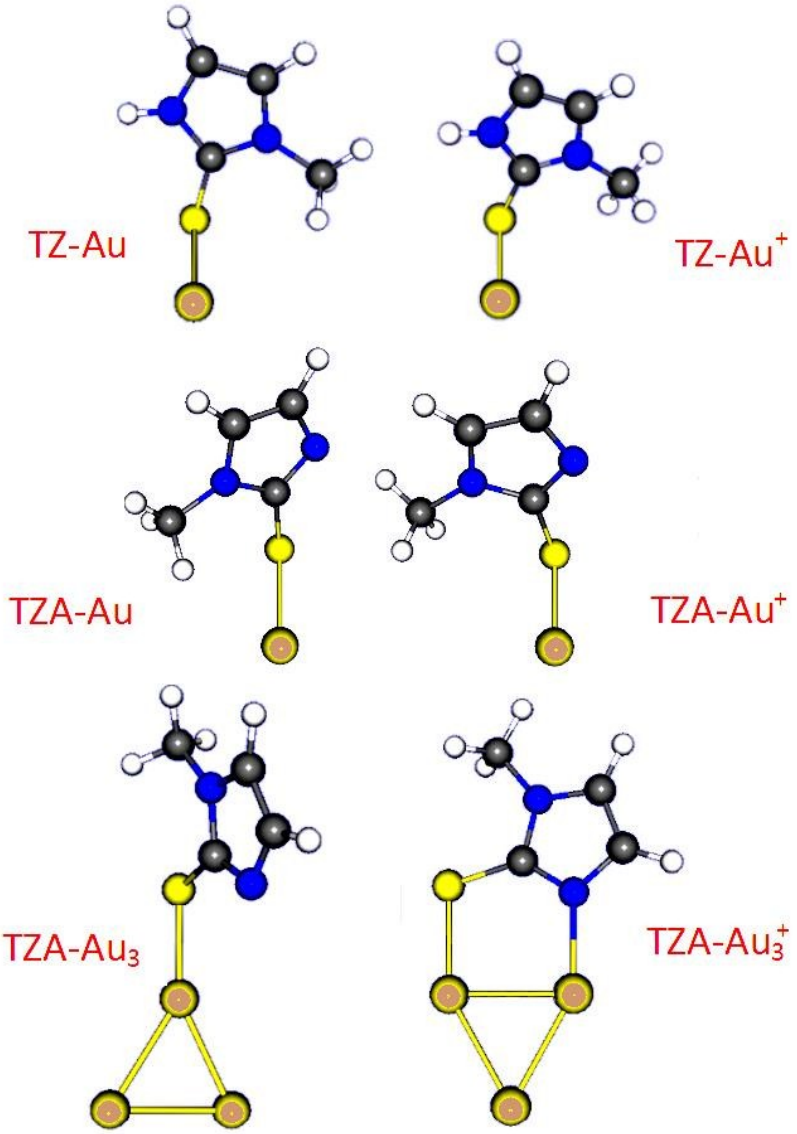

Fig. 4 – DFT-optimized structures of the ligand/metal complexes used to model the interaction of methimazole with the gold nanoparticles.

View Article Online
DOI: 10.1039/C5CP07597A

In order to take into account the possibility that both sulfur and nitrogen atom interact with the metal oxide, we have also considered clusters formed by three gold atoms. Moreover, adatoms and adclusters may consist of neutral atoms Au(0) or contain also Au(I). Actually, the study of the XPS spectra evidences the presence of oxidized gold as Au(I) on the surface of the gold nanoparticles, even if very minority, less than 10% in comparison with the Au(0) content (see **Fig. 5**); the fitting of the 4f doublet requires at least two components, whose binding energy values, around 83 and 85 eV, are in good agreement with metallic gold and Au (I), respectively.[35,36]

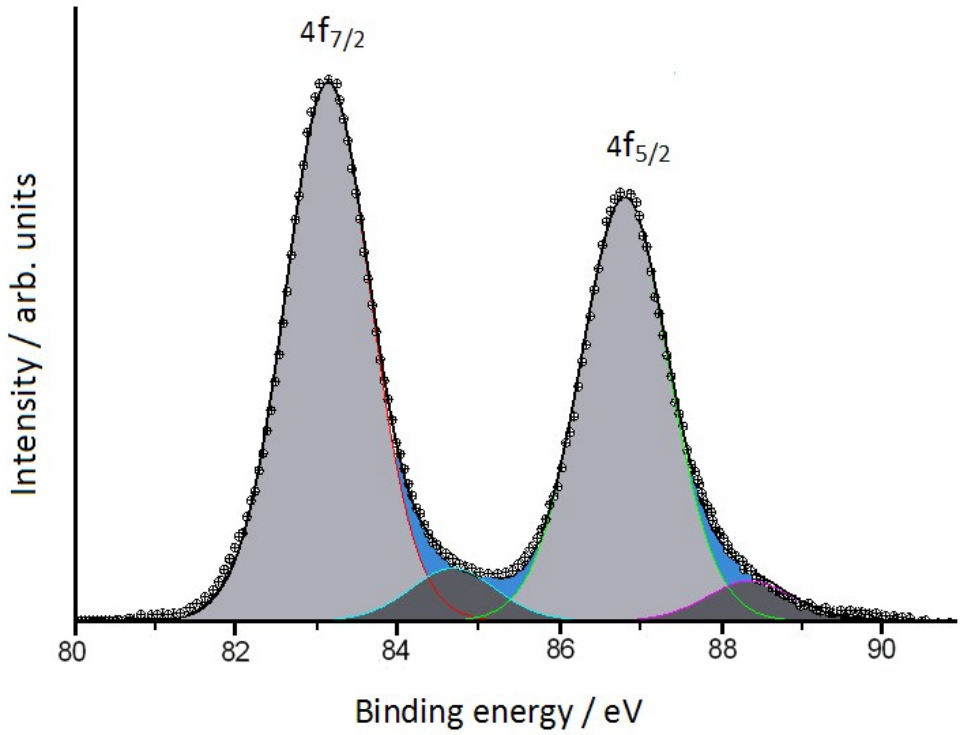

Fig. 5 – Deconvolved XPS spectrum of deposited Au nanoparticles ($4f_{7/2}$ and $4f_{5/2}$ transitions). Circles represent experimental points, while light gray and dark gray the contributions of Au(0) and Au(I), respectively.

View Article Online
DOI: 10.1039/C5CP07597A

As shown in **Fig. 4,** both TZA-Au and TZA-Au^+ models show the binding of the thiolate anion with gold only through the sulfur atom; this fact was expected by considering that in the thiolate anion the calculated negative charge of the sulfur atom results much larger than that of the ring nitrogen atom (see **Table S2, ESI**). As concerning the models with thiolate bound to gold clusters, only the TZA-Au_3^+ model foresees a bidentate bond of the gold cluster with both sulfur and nitrogen. The agreement between SERS and calculated wavenumbers is satisfactory in the case of the TZA-Au and TZA-Au_3 complexes, as shown in **Table 1**, while the other models are less effective in reproducing the positions of the SERS bands (see **Table S3, ESI**), especially regarding the strongest SERS band at 1367 cm^{-1}, for which the calculated wavenumbers are too low or too high if compared with the observed value. Moreover, the efficiency of the TZA-Au and TZA-Au_3 complexes, where thiolate is bound to gold only through the sulfur atom, in reproducing the SERS frequencies could explain the evidence of few significant frequency-shifts with respect to the Raman spectrum in alkaline solution. In fact, most of the observed Raman bands are due to ring and methyl deformations (see **Fig. S2, ESI**); hence, they are scarcely affected by the interaction with the metal that involves only the sulfur atom as a substituent bound to the ring.

But is the comparison between the simulated and experimental spectra shown in **Fig. 6**, which clearly indicates that the model TZA-Au is definitely the most suitable to reproduce completely the SERS spectrum, including band positions and relative intensities. In fact, even if also the TZA-Au_3 model provides a spectral profile in good agreement with the experimental one, the strongest band results markedly up-shifted if compared with that SERS observed at 1367 cm^{-1}; in addition, the band corresponding to that observed around 1324 cm^{-1} is too weak with respect to the experimental one. The failure of all the models that consider gold adatoms or adclusters with

View Article Online
DOI: 10.1039/C5CP07597A

positive charges is consistent with the XPS results, which show that on the surface of the gold nanoparticles the species Au(I) is very minority compared to the species Au(0).

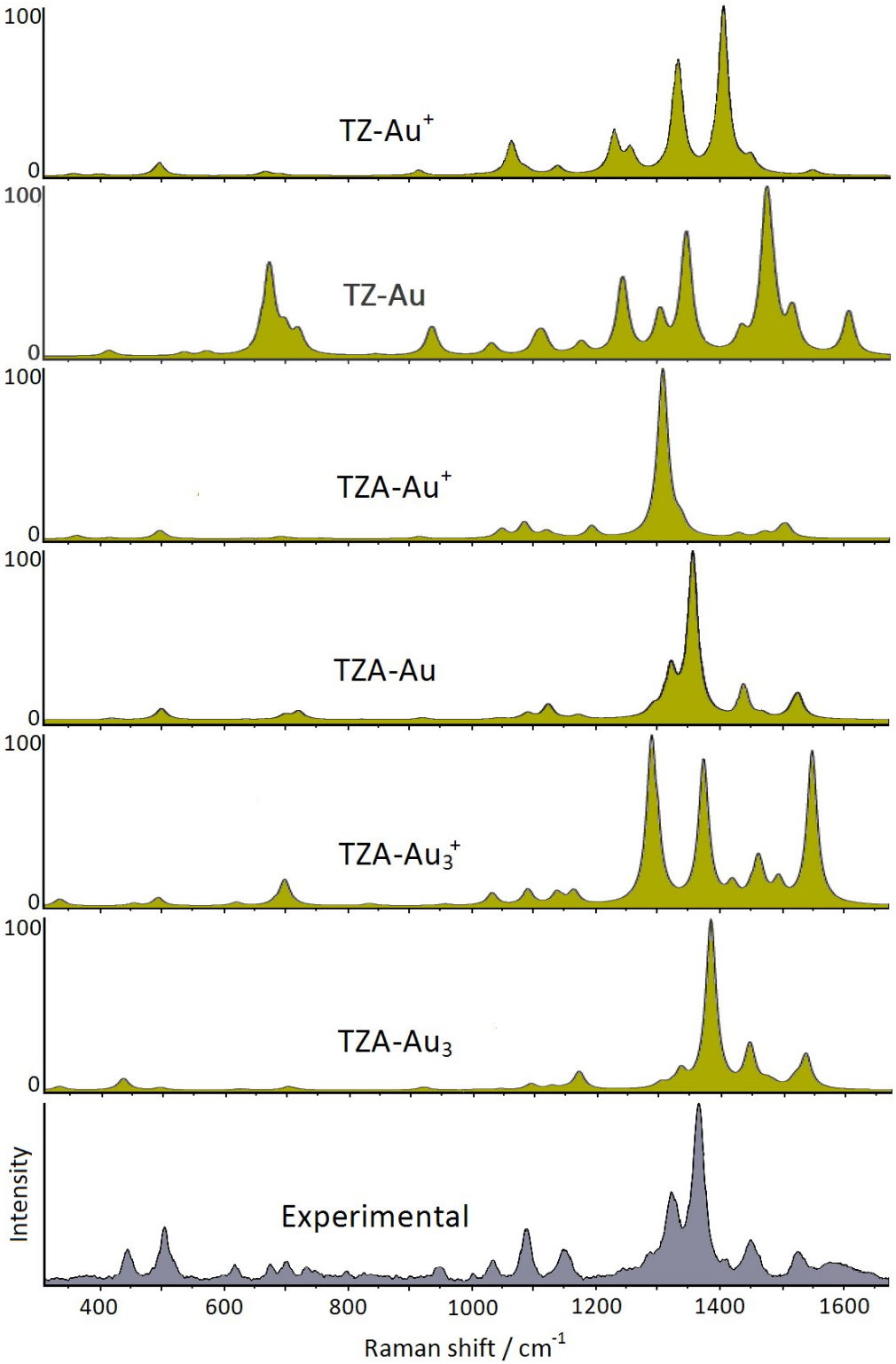

View Article Online
DOI: 10.1039/C5CP07597A

Fig. 6 – Simulated SERS spectra of different model systems, compared with the observed SERS spectrum (647.1 nm laser excitation).

In this regard, it should be noted that the prominent SERS bands correspond to ring deformation modes, mixed with the C-S bond stretching, as shown in **Fig. 7**. Only the vibration corresponding to the SERS band around 500 cm^{-1} shows a significant change of the Au-S bond distance; thus, according to selection rules of the molecule-metal charge-transfer,[37] a marked SERS enhancement is expected with respect to the corresponding Raman band observed at 503 cm^{-1}, as well as found experimentally (**Fig. 2**).

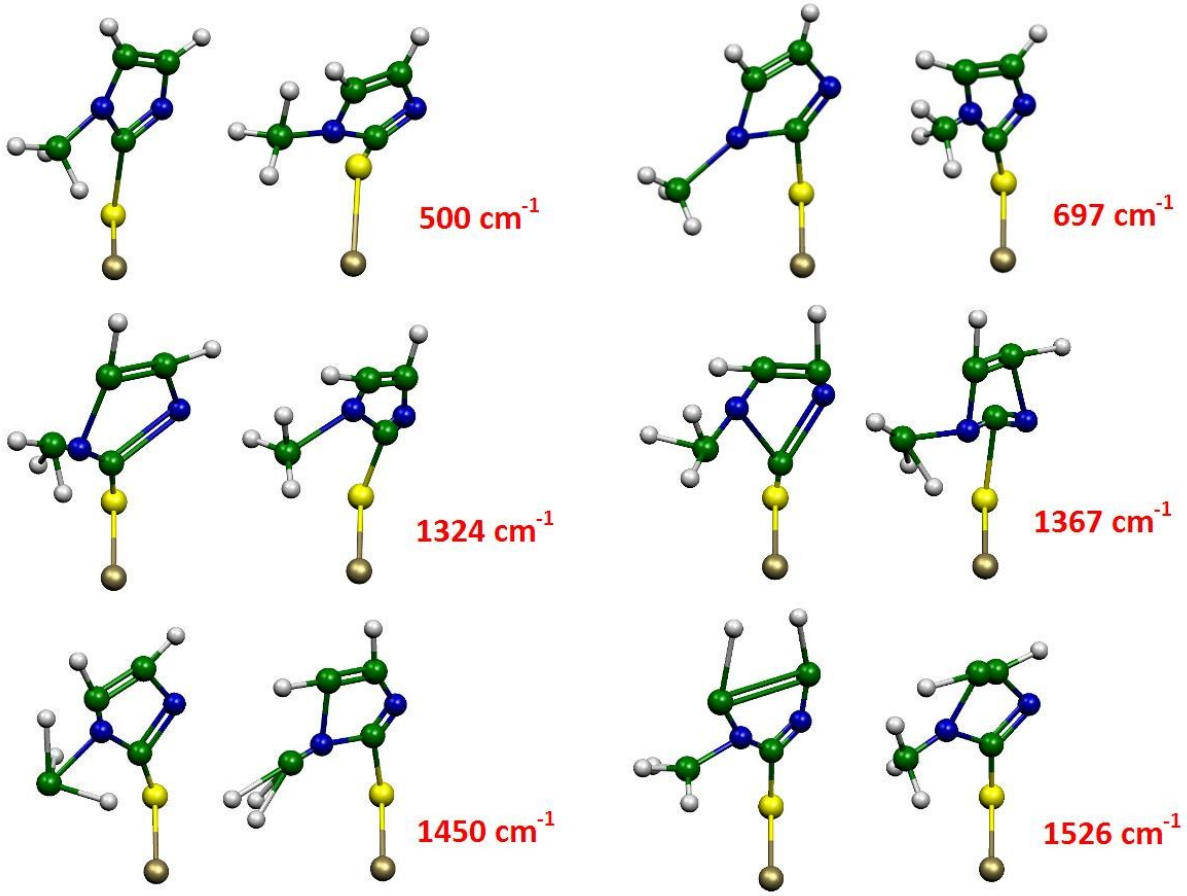

View Article Online
DOI: 10.1039/C5CP07597A

Fig. 7 – Normal modes calculated for the TZA-Au model in the maximum deformations, corresponding to the prominent SERS bands.

Finally, there is to discuss the low-frequency region (100-300 cm^{-1}) of the SERS spectrum. As shown in **Fig. 8**, a broad band appears at about 200 cm^{-1}; it is attributable to the stretching vibration of the Au-S bond, since in this region neither the molecule nor the colloid without ligand shows bands. On the other hand, Au-N stretching bands are expected at higher frequencies, as observed in the SERS spectra of 1,2,3-triazole adsorbed on colloidal gold.[38] Actually, the DFT calculations for the TZA-Au model indicate the occurrence of a band at 199 cm^{-1}, attributable to the Au-S stretching mode, mixed with the ring torsion around the C-S bond, as shown in **Fig. 8**. Also this result confirms that the ligand molecules are really chemisorbed on the Au nanoparticles as thiolate anions bound to the gold surface exclusively through the sulfur atoms.

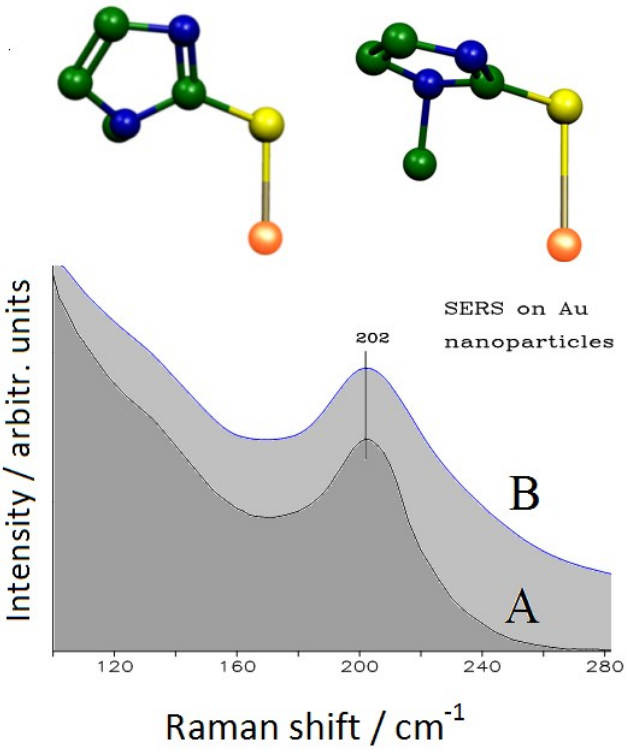

View Article Online
DOI: 10.1039/C5CP07597A

Fig. 8 – Low-frequency SERS spectra (A: exc. 647.1-nm; B: exc. 1064-nm) of TZ in Au colloid. The normal mode calculated at 199 cm^{-1} for the TZA-Au model is shown above for the two maximum deformations (hydrogen atoms hidden).

Conclusions

In conclusion, the SERS study of methimazole adsorbed on gold colloidal nanoparticles has shown the possibility of using the Raman excitation also in the NIR spectral region, i.e. in the skin transparency window where generally no fluorescence emission occurs. This paves the way to the use of the SERS technique to observe the Raman signal in biological environment. The DFT approach has been particularly useful to identify the molecular species, the thiolate anion, which chemically interacts with the active sites of the gold surface, modeled as zero-charge metal adatoms. From the comparison of the simulated Raman spectra of different surface complexes with the experimental SERS spectra it has been also possible to argue that the ligand interacts with the metal only through the sulfur atom. This result can be important for the use of TZ@Au nanohybrids in the process of drug delivery. Actually, it was proved that the Au-S bonds in organothiols adsorbed on gold nanoparticles can be broken by action of iodide anions;[39] in this way, the TZ molecules could be released there where used as antithyroid drug.

Electronic Supplementary Information (ESI) available: other computational details.

Ackowledgments

FMM's post-doctoral position at UniMORE is supported by the Italian "*Ministero dell'Istruzione, dell'Università e della Ricerca*" (MIUR) through the "*Futuro in Ricerca*" (FIRB)

View Article Online
DOI: 10.1039/C5CP07597A

Grant RBFR1248UI_002 entitled “Novel Multiscale Theoretical/Computational Strategies for the Design of Photo and Thermo responsive Hybrid Organic-Inorganic Components for Nanoelectronic Circuits”. The authors gratefully thank Dr. Stefano Caporali for the XPS measurements.

View Article Online
DOI: 10.1039/C5CP07597A

Table 1 – Experimental Raman shifts (cm^{-1}) of TZ compared with the DFT-calculated vibrational wavenumbers.

Raman alkaline solution	Calc. TZA	SERS on gold excitation: 1064 nm	SERS on gold excitation: 647.1 nm	Calc. TZA-Au	Calc. TZA-Au_3
	243			241	234
	272			278	337
	421	440 m	441 m	420	438
503 w	511	500 s	500 s	500	498
596 vvw	596				
622 vw	628	614 w	615 w	635	627
		672 w	672 w	667	659
694 s	699	695 w	697 w	698	702
	722	730 vw	731 vw	720	715
	808	826 vvw	822 vvw	823	834
925 w	909	945 w	943 w	921	921
1030 vvw	1030	1032 w	1033 w	1046	1044
1083 m	1081	1086 m	1088 s	1091	1093
	1098				
1123 w				1125	1127
1147 vw	1151	1145 m	1147 m	1151	1149
	1171			1174	1171
1283 sh	1279		1287 w	1295	1303
1302 s	1306	1322 s	1324 m	1322	1333
1361 vs	1357	1367 vs	1367 vs	1357	1381
1414 w	1418				
1447 vw	1458	1452 s	1450 s	1440	1444
1475 vvw	1494			1469	1471
				1472	1482
	1500			1519	1517
1523 s	1537	1525 m	1526 m	1528	1534

View Article Online
DOI: 10.1039/C5CP07597A

REFERENCES

(1) B. Merchant, J. F. Lees and W. D. Alexander, *Pharmacol. Ther. Part B*, 1978, **3**, 305-348.

(2) A. P. Weetman, A. M. McGregor and R. Hall, *Clin. Endocrinol*., 1984, **21**, 163-172.

(3) P. Kendall-Taylor, *Br. Med. J.*, 1984, **288**, 509-511.

(4) K. A. Woeber, *Endocr. Pract*., 2002, **8**, 222-224.

(5) M. Garner, D.R. Armstrong, J. Reglinski, W. E. Smith, R. Wilson, and J. H. McKillop, *Bioorg. Med. Chem. Lett*., 1994, **4**, 1357-1360.

(6) R. Heidari, H. Babaei, L. Roshangar and M. A. Eghbal, *Adv. Pharm. Bull.*, 2014, **4**, 21-28.

(7) K. Bahrami, P. Nazari, M. Nabavi, M. Golkar, A. Almasirad and A. R. Shahverdi, *Nanomedicine J.*, 2014, **1**, 155-161.

(8) M. Demurtas and C. C. Perry, *Gold Bull*, 2014, **47**, 103–107.

(9) L. A. Austin, M. A. Mackey, E. C. Dreaden and M. A. El-Sayed, *Arch. Toxicol.*, 2014, **88**, 1391-1417.

(10) V. P. Torchilin, *Nat. Rev. Drug Disc*., 2014, **13**, 813-827.

(11) S. Schlücker, *Surface Enhanced Raman Spectroscopy: Analytical, Biophysical and Life Science Applications*, Wiley-VCH, Weinheim, 2011.

(12) A. R. Owen, J. W. Golden, A. S. Price, W. A. Henry, W. K. Barker and D. A. Perry, *J. Phys. Chem. C*, 2014, **118**, 28959-28969.

(13) M. Pagliai, S. Caporali, M. Muniz-Miranda, G. Pratesi and V. Schettino, *J. Phys. Chem. Lett.*, 2012, **3**, 242-245.

(14) M. Muniz-Miranda and M. Pagliai, *J. Phys. Chem. C*, 2013, **117**, 2328-2333.

(15) J. Turkevich, P. C. Stevenson and J. A. Hillier, *Discuss. Faraday Soc*., 1951, **11**, 55-75.

(16) M. J. Frisch *et al.*, Gaussian 09, Revision D.01. Gaussian, Inc., Wallingford.

(17) A. D. Becke, *J. Chem. Phys*., 1993, **98**, 5648-5652.

(18) C. Lee, W. Yang and R. G. Parr, *Phys. Rev. B*, 1988, **37**, 785-789.

(19) F. Weigend and R. Ahlrichs, *Phys. Chem. Chem. Phys*., 2005, **7**, 3297-3305.

View Article Online
DOI: 10.1039/C5CP07597A

(20) S. H. Vosko, L. Wilk and M. Nusair, *Can. J. Phys*., 1980, **58**, 1200–1211.

(21) P. J. Stephens, F. J. Devlin, C. F. Chabalowski and M. J. Frisch, *J. Phys. Chem.*, 1994, **98**, 11623–11627.

(22) N. Maiti, S. Thomas, J. A. Jacob, R. Chadha, T. Mukherjee and S. Kapoor, *J. Coll Interface Sci.*, 2012, **380**, 141–149.

(23) R. L. Birke, V. Znamenskiy and J. R. Lombardi, *J. Chem. Phys.*, 2010, **132**, 214707.

(24) M. Muniz-Miranda, C. Gellini, M. Pagliai, M. Innocenti, P. R. Salvi and V. Schettino, *J. Phys. Chem. C*, 2010, **114**, 13730-13735.

(25) N. Biswas, S. Thomas, A. Sarkar, T. Mukherjee and S. Kapoor, *Chem. Phys. Lett.*, 2009, **479**, 248–254.

(26) F. Muniz-Miranda, M. C. Menziani and A. Pedone, *J. Phys. Chem. C*, 2014, **118**, 7532–7544.

(27) F. Muniz-Miranda, M. C. Menziani and A. Pedone, *J. Phys. Chem. A*, 2015, **119**, 5088–5098.

(28) E. S. Raper, J. A. Creighton, R. E. Oughtred, and I. W. Nowell, *Acta Cryst. B*, 1983, **39**, 355-360.

(29) D. P. Hanlon and S. Shuman, *Experientia*, 1975, **31**, 1005-1006.

(30) S. Saha, R. K. Roy and P.W. Ayers, *Int. J. Quantum Chem*., 2008, **109**, 1790-1806.

(31) H. M. Zakaria, A. Shah, M. Konieczny, J. A. Hoffmann, A. J.Nijdam and M. E. Reeves, *Langmuir,* 2013, **29**, 7661-7673.

(32) W. Huang, J.-Z. Jiang, L. Chen, B.-Q. Zhang, S.-F. Deng, J. J. Sun and W.-K. Chen, *Electrochim. Acta*, 2015, ***164***, 132-138.

(33) M. Muniz-Miranda, F. Muniz-Miranda and S. Caporali, *Beilstein J. Nanotechnol*., 2014, **5**, 2489-2497.

(34) M. Pagliai, F. Muniz-Miranda, V. Schettino and M. Muniz-Miranda, *Progr. Colloid Polymer Sci*., 2012, **139**, 39-44.

(35) J. F. Moulder, W. F. Stickle, P. E. Sobol and K. D. Bomben, *Handbook of X-ray Photoelectron Spectroscopy*; Perkin-Elmer Corporation, Eden Prairie, 1992.

(36) J.-P. Sylvestre, S. Poulin, A. V. Kabashin, E. Sacher, M. Meunier and J. H. T. Luong, *J. Phys. Chem. B*, 2004, **108**, 16864-16869.

View Article Online
DOI: 10.1039/C5CP07597A

(37) J. A. Creighton, in *Spectroscopy of Surfaces*; Clark, R. J. H.; Hester, R. E., Eds.; Wiley, Chichester, 1988; pp 37-85.

(38) B. Pergolese, M. Muniz-Miranda and A. Bigotto, *J. Phys. Chem. B*, 2004, **108**, 5698-5702.

(39) G. S. Perera, A. LaCour, Y. Zhou, K. L. Henderson, S. Zou, F. Perez, J. P. Emerson and D. Zhang, *J. Phys. Chem. C*, 2015, **119**, 4261-4267.

View Article Online
DOI: 10.1039/C5CP07597A

Table of Contents (TOC) Image

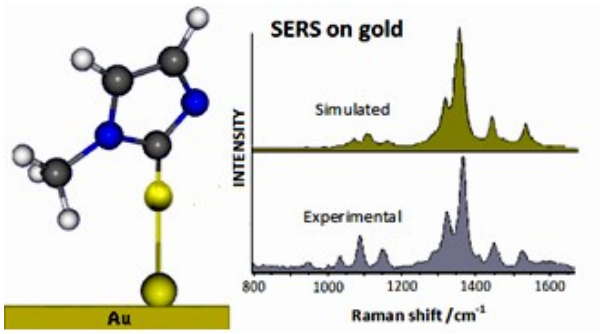

The SERS/DFT study of methimazole chemisorbed on Au nanoparticles paves the way to the use of these nanohybrids in biomedicine.